Supplementary Information (SI) for Nanoscale Horizons.

Mechanism of Oxygen Reduction via Chemical Affinity in NiO/SiO_2 Interfaces Irradiated with keV Energy Hydrogen and Helium Ions for Heterostructure Fabrication

Mario Mery,[*,†] Claudio Gonzalez-Fuentes,[‡,¶] Igor Stanković,[*,§] Jorge M. Nuñez,[‖,⊥,#] Jorge E. Valdés,[†] Myriam H Aguirre,[‖,⊥,#] and Carlos García[*,¶]

†*Atomic Collisions Laboratory, Physics Department, Universidad Técnica Federico Santa María, Valparaíso, Chile*

‡*Instituto de Física, Pontificia Universidad Católica de Chile, Santiago, Chile*

¶*Physics Department, Universidad Técnica Federico Santa María, Av. España 1680, Valparaíso, Chile*

§*Scientific Computing Laboratory, Center for the Study of Complex Systems, Institute of Physics Belgrade, University of Belgrade, Pregrevica 118, 11080 Zemun, Serbia*

‖*Dept. Física de la Materia Condensada, Universidad de Zaragoza, Pedro Cerbuna, 12, 50009, Zaragoza*

⊥*INMA-Instituto de Nanociencia y Materiales de Aragón- CSIC, Mariano Esquillor s/n, 50018, Zaragoza*

#*LMA- Laboratorio de Microscopías Avanzadas, Universidad de Zaragoza, Mariano Esquillor s/n, 50018, Zaragoza*

E-mail: mario.mery@usm.cl; igor.stankovic@ipb.ac.rs; carlos.garcia@usm.cl

Supplementary Material

Experimental

Sample preparation

The thin films were deposited by magnetron sputtering onto Si -100- substrates in a vacuum chamber pumped down to a $1.5x10^{-9}$ mbar initial pressure. The NiO 45 nm thin films were deposited from a 99.99% purity NiO sputtering target with a deposition rate of 0.17 Å/s. The 45 nm thickness of NiO was measured by TEM with a cross-sectional image of the sample and compared with the value obtained from the quartz microbalance during thin film fabrication. The 170 nm NiO films were made from 100 nm thick pure Ni sputtered films which were subsequently subjected to thermal oxidation by heating the sample holder up to 480° C at atmospheric conditions. The Ni thickness is measured using a quartz microbalance. After that, the sample is heated to get NiO by thermal oxidation. The 170 nm of NiO is extrapolated from the swelling caused by thermal oxidation and estimated by SEM. The NiO (or Ni) thin film is deposited on a unique Si wafer 4 inch. All the samples used in this experiment came from this unique NiO/Si wafer. The samples were cut with a diamond-tipped pencil from the NiO/Si wafer. The same procedure is used to fabricate the 170 nm NiO. All measurements are performed at room temperature.

Ion irradiation

The irradiation was performed using ion beams of He^+ and H^+ impinging perpendicularly to the NiO thin films surface. The ion beams were produced by a hot discharge source using high-purity H_2^+ and He^+ gas which are accelerated to 10 keV. The hydrogen beam was mass analyzed by a Wien filter, and the molecular states of H_2^+ are selected, the H^+ and H_3^+ are deflected out of the beam line. The ion flux intensity is in the range of 0.1-1 A/m^2, and the ion beam spot size is 1 mm^2 circular shape. The NiO samples were placed in front of

the beam and mounted on a sample holder attached to a five-axis precision manipulator. For hydrogen molecules, it is well-known that molecular dissociation occurs when passing through the first monolayer of the material, resulting in two protons traveling independently with half of the initial energy. The charged particle energy is measured using a 166° spherical sector electrostatic energy analyzer with a resolution of better than 1%. The current on the sample was measured using a picoammeter biased at 50 Volt to collect the secondary electron. The irradiation chamber was evacuated by turbo molecular and ion pumps. The operating pressure of the ion gun chamber was 5×10^{-6} Torr and the irradiation of the samples was made in the collision chamber at a pressure of around 5×10^{-9} Torr. All irradiation experiments were carried out at room temperature. The increase of temperature of the samples was not observed during irradiation.

We used the 170 nm NiO sample to study the effect of sputtering in the film under high-fluence He ion irradiation. During this process, substantial sputtering occurs, which reduces the film's thickness. Consequently, to compensate for this sputtering effect, the initial thickness of the film must be increased.

Magnetometry

MOKE. Longitudinal Magneto-Optical Kerr Effect (MOKE) magnetometry was employed to probe the magnetic response of the irradiated NiO. The configuration employed was the nearly crossed polarizers condition with an incidence angle of 63 deg. The measurements were performed at room temperature in the range of the magnetic field from -300 Oe to 300 Oe. We quantify the size of the MOKE response as the difference of the MOKE signals between positive and negative fields of saturation. **SQUID**. Magnetization at saturation was obtained from M-H curves by using a superconducting quantum interference device (SQUID) magnetometer (SQUID - VSM based MPMS System, Quantum Design-make). Magnetization is recorded as a function of the magnetic field in the range of 4kOe$\leq H \leq -$4kOe at room temperature.

Ni thickness determination from SQUID measurements

We determine the thickness of the Ni film induced by irradiation as follows: first, we measured the magnetization of saturation of a reference sample of Ni, 50 nm thickness, with known volume and density. Dividing the saturation of magnetization by the total mass of the Ni film, we obtained the specific saturation of magnetization (M_e), giving 53.6 emu/g for the reference sample. Following, we measured the saturation of magnetization (M_s) of the irradiated samples. and the thickness T of the irradiated film is determined using the following relation:

$$T = \frac{M_s}{M_e \cdot D \cdot A} \tag{1}$$

where M_e is the specific saturation of magnetization of the reference sample, D is the density of Ni, and M_s is the saturation of magnetization of the irradiated sample. A is the area of the samples, which has been completely irradiated over its surface. To obtain the M_s the diamagnetic component from the silicon substrate has been subtracted for each hysteresis cycle. Hence, the NiO samples, irradiated with He^+ and H^+, have a saturation magnetization of M_s =5.5 and 22.1 emu, respectively. This is equivalent to a Ni thickness of 5.1 and 20.6 nm, for the samples irradiated with H^+ and He^+, respectively. The M-H curves for all samples exhibited the characteristic hysteresis of ferromagnetic materials.

Elemental analysis and crystal structure

EDS-SEM. The elemental composition of the samples was characterized using a field-emission scanning electron microscope (FE-SEM, S-4700, Hitachi) with an energy-dispersive X-ray spectroscope. The energy dispersive X-ray analysis (EDAX) measurements were conducted onto the irradiation region of the sample and the stoichiometry of the specimens is calculated by atomic% for Ni and O. We use an electron beam of 2 kV, hence the k-lines are evaluated. **EDS in TEM**. Two EDAX measurements were performed for each sample, across a total of four samples: unirradiated, two irradiated with He^+, and one with H^+. Both

lines taken for He^+ irradiated samples indicate a similar amount of NiO reduction at the interface. High resolution Scanning Transmission Electron Microscopy with a High Angular Annular Dark Field Detector (HRSTEM-HAADF) was performed using a FEI Titan G2 microscope with a probe corrector and in Tecnai F30 from FEI at 300 keV. In-situ chemical analysis was performed using Energy-dispersive Spectroscopy (EDS). Lamella samples for TEM were prepared by Focused Ion Beam (FIB) in Helios 650 dual beam equipment. Only (200) Ni planes (0.175 nm) are considered to distinguish Ni grains from NiO grains. The reason for not considering the planes of NiO [200] and Ni [111] in the analysis is due to their similar interplanar distance, with values of 0.2085 nm and 0.2034 nm, respectively. This similarity makes it very difficult to differentiate between them.

Computer simulation

The diffusion coefficient of oxygen D_{O}^{x} is a local property reflecting evolving chemical and structural properties of the material along the diffusion profile, while diffusion coefficients of nickel and silica species are assumed to be homogeneous. To model absorption of oxygen through the chemical bonding of oxygen with silica we also introduce a unidirectional mass transfer of oxygen at the interface point ($x = 0$) between nickel oxide NiO and silica Si written generically $I_{\mathrm{O}}^{x=0} = cu^{x=0+}$ with $c = 5 \cdot 10^{-11}$ m/s. Here we have a model governed by a system of partial differential equations with different diffusion rates and absorption of oxygen into silica. The grid will be equally distributed if the distance between grid cells satisfies the spatial equidistribution equation over

$$\int_{x_{i-1/2}}^{x_{i+1/2}} n^x(u)\,dx = \int_{x_{i+1/2}}^{x_{i+3/2}} n^x(u)\,dx = \mathrm{C}, \quad i = 1, \ldots, N_c, \tag{2}$$

which can be written in a discrete form as:

$$N_i \Delta x_i = N_{i+1} \Delta x_{i+1} = \mathrm{C}, \quad i = 1, \ldots, N_c, \tag{3}$$

where $\Delta x_i = x_{i+1/2} - x_{i-1/2}$ is the local size of the cell, N_i is a discrete approximation of the molar density in the cell size, and C is a constant.

Figure 5a of the report shows the diffusion coefficient obtained from the Kinchen-Peace model. In this model, equation 1 gives the magnitude of the diffusion coefficient, and Eq. 3 is written so that P(x) is the number of displacements per target atom per unit time.

$$P(x) = \frac{0.8}{2NE_{\mathrm{d}}} \left(\frac{\mathrm{d}E}{\mathrm{d}x}\right)_n \phi \tag{4}$$

Here, ϕ is the ion flux, N is the atomic density of the solid, E_d is the effective threshold displacement energy, λ is the root-mean-square separation for a vacancy-interstitial pair, and $(dE/dx)_n$ is the ion energy deposited per unit depth into atomic processes (figure 4b in the main text). The specific values of each of the variables are specified in the following table:

Table S1: The table specifies the parameters to determine the diffusion coefficient according to the Kinchen-Peace model

λ	1.5 nm
N	5,22 x10^{22} atom/cm^3
E_d	30 eV
ϕ	10^{18} ion/cm^2
Irradiation time	5000 s

The mechanisms of ion-induced diffusion may be distinguished as follows. First, atoms move as a result of nuclear energy transfer as the ion beam particles traverse the lattice, an effect frequently referred to as cascade mixing. Second, mobile point defects generated by irradiation may undergo extensive diffusion before annihilation or agglomeration, causing enhanced atomic diffusion. Finally, extended defects such as dislocations are produced by defect agglomeration, and these may provide paths for rapid diffusion. As a result, the increased ion energy transfer in the region of Bragg´s peak maximum would lead to an increased reduction of NiO into pure Ni. In the proposed framework, the reduction of NiO results in a positive loop, concentrating absorption of ion energy in nickel-rich areas while almost four times lighter oxygen will diffuse faster after adsorbing the ion energy in the

interface region. In the case of irradiation with helium, the energy transfer showed a much weaker dependence on depth. Therefore we studied a systems in which the He^+ induced diffusion coefficient was independent of the depth, $D_2 = 2 \cdot 10^{-16}\text{cm}^2/\text{s}$, and another in which the H^+ induce diffusion coefficient is linearly dependent on nickel amount between $D_1^{\text{Ni}} = 1 \cdot 10^{-15}\text{cm}^2/\text{s}$ and $D_1^{\text{NiO}} = 2 \cdot 10^{-16}\text{cm}^2/\text{s}$, for pure nickel and nickel oxide, respectively. As observed, the diffusion coefficient for a helium irradiated system does not depend on chemical composition, while for irradiation with hydrogen, the diffusion coefficient depends on the Ni and O concentration, following the relation $D_1(n_{\text{Ni}}, n_{\text{O}}) = D_1^{\text{NiO}} + D_1^{\text{Ni}}\dot{(}1 - 2n_{\text{Ni}}/(n_{\text{Ni}} + n_{\text{O}}))$. To model absorption of oxygen through the chemical bonding of oxygen with silicon, we also introduce a unidirectional mass transfer of oxygen at the interface point ($x = 0$) between nickel oxide NiO and silica Si written generically $I_{\text{O}}^{x=0} = cu^{x=0+}$ with $c = 2 \cdot 10^{-10}$ m/s. The diffusion rate of nickel is chosen to be smaller based on its five times larger mass difference to oxygen $1 \cdot 10^{-16}\text{cm}^2/\text{s}$ and silicon the same $1 \cdot 10^{-16}\text{cm}^2/\text{s}$, cf. Ref.[1,2]

It is observed that the diffusion coefficient calculated by the Kinchen-Peace model, induced by hydrogen irradiation (figure 5 in the main text), is an order of magnitude lower than the diffusion coefficient of the computational simulation which reproduces well the experimental results. On the other hand, the diffusion coefficient induced by He is well described by the Kinchen-Peace model. This difference is because the Kinchen-Peace model does not consider the chemical interaction between the hydrogen ion and the oxygen atom, and only considers ballistic collisions, like hard-spheres.

Stopping Range of Ions in Matter (SRIM) Calculation Information

Figures S1 and S2 show the results of SRIM calculations for 5 keV proton and 10 keV He ion irradiation on the NiO/Si target. These calculations were performed using a Surface Sputtering/Monolayer Collisions routine with 200,000 ions. The target composition was taken as Ni (50 atomic %), and O (50 atomic %), with a density of 6.67 g/cm3. The NiO target layer was kept at a thickness of 45 nm. The substrate composition was taken as Si

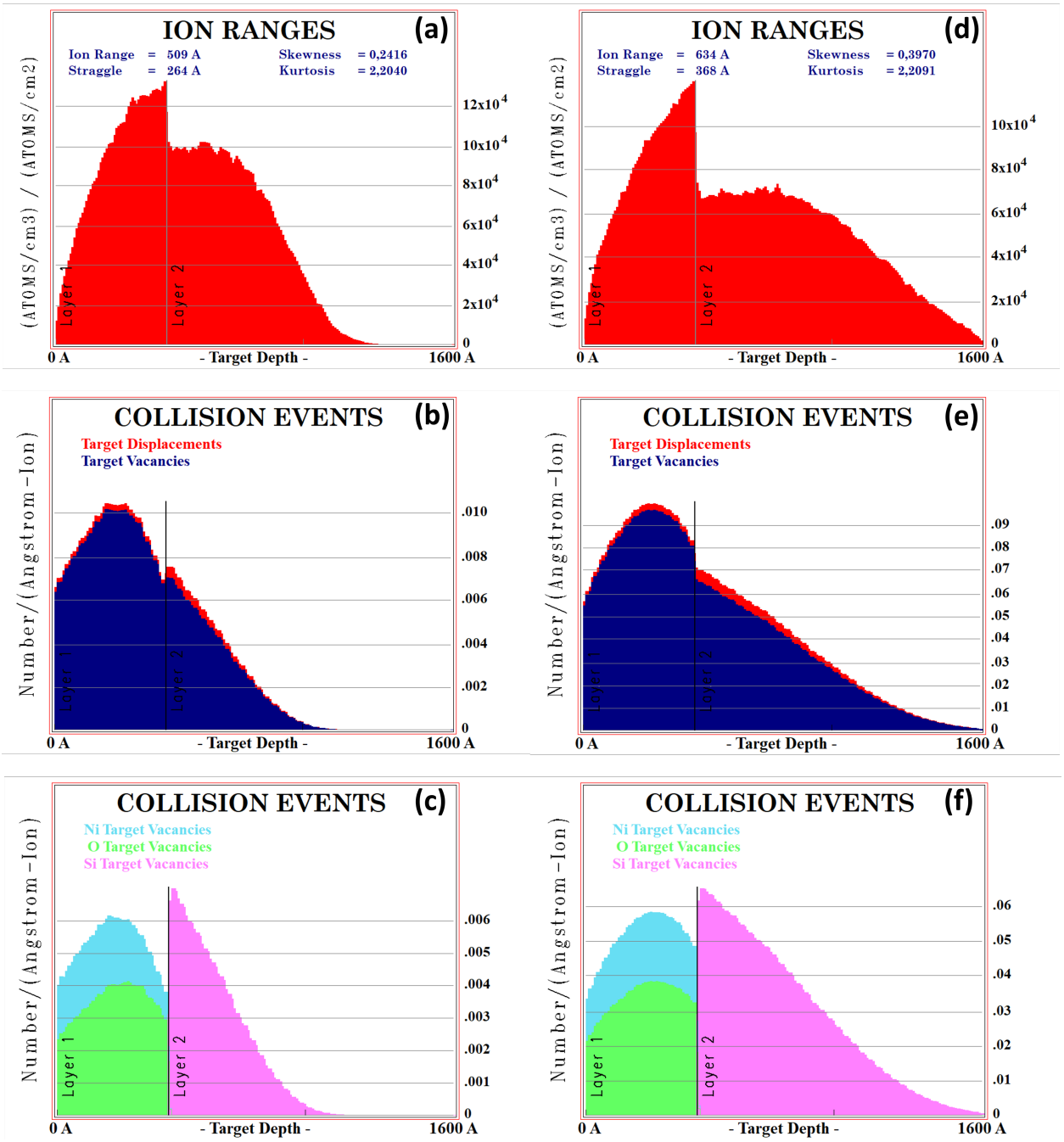

Figure S1: TRIM simulated distribution of protons (a) and He (b) as a function of target depth. (b) and (e) show the number of vacancies and displacements per atom as a function of target depth for H and He respectively. (c) and (d) show the vacancy of Ni (light-blue), oxygen (green), and Si (pink) as a function of target depth.

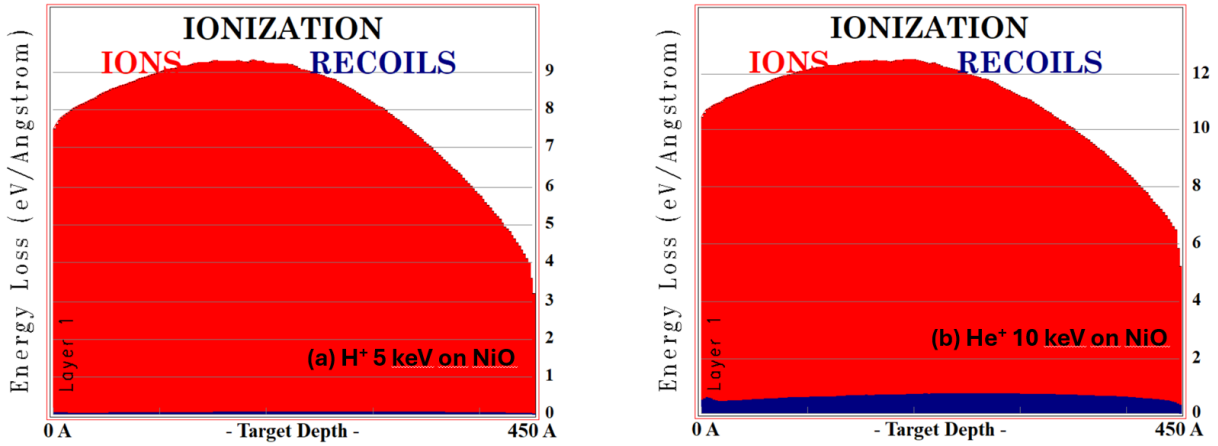

Figure S2: The graph show the energy loss (eV/Å) as a function of penetration depth. (a) displays the energy loss for H^+ and (b) for He^+ impinging on NiO. The area under the curve represents the energy transferred to the target electrons. The red area data, labeled "Ions," indicates the direct energy transferred from the ion to the target electrons. The blue area data, labeled "Recoils," indicates the energy transferred from recoiling target atoms to the target electrons.

100%, with a density of 2.39 g/cm3. In the SRIM calculation, for the target atoms (Ni, O and Si) displacement, energy of 25 eV, 28 eV, and 17 eV was considered to estimate the damages.

Following SRIM simulations, the sputtering yield of NiO by hydrogen bombardment is 0.021 atom/ion, and by He^+ bombardment is 0.27 atoms/ion. The relative sputtering yield for O and Ni by H^+ bombardment on a NiO matrix are 0.0135 atom/ion and 0.0075 atom/ion, respectively. The relative sputtering yield for O and Ni by He^+ bombardment on a NiO matrix is 0.171 atom/ion and 0.099 atom/ion for oxygen and nickel respectively. The rate of Ni and O relative sputtering (Ni/O) is 0.58 for He and 0.56 for hydrogen. That means the relative sputtering of Ni and O in NiO by irradiation of H and He ions, should be in the same proportion, according to TRIM. On the other hand, ion irradiation can generate defects in the material, such as vacancies and dislocations, which can enhance the atomic diffusion in the material. Defects can increase the rate of diffusion due to the increased number of vacancy sites and provide pathways for rapid atomic displacement. Theoretical models consider that the diffusion on materials is proportional to the number of vacancies.[3]

It is important to note that the effects of irradiation on diffusion depend on many factors, such as irradiation energy and dose, temperature, and material composition.[4] According to SRIM simulations, hydrogen irradiation on NiO induces an average vacancy of 9×10^{-3} vacancy/Å·ion, while He irradiation induces an average vacancy almost 10 times higher, i.e. 9×10^{-2} vacancy/Å·ion (Fig. 2S b-f). In addition, the SRIM simulations show that the oxygen defects and vacancies are 40% lower than Ni vacancies, these are observed with H and He irradiation (Figure 2S). Following the SRIM calculation, He removes oxygen and Ni practically at the same rate as hydrogen, and the generation of vacancies is higher for He in comparison with hydrogen, which is opposite to what we observed experimentally in this work. That is explained because the sputtering calculation of SRIM only considers pure ballistic recoil mechanism in an amorphous target (or physical collision). Therefore, other mechanisms of oxygen removal must be considered, such as diffusion and chemical interactions.

References

(1) Atkinson, A.; Taylor, R. I. The self-diffusion of Ni in NiO and its relevance to the oxidation of Ni. *Journal of Materials Science* **1978**, *13*, 427–432.

(2) Schweigert, I. V.; Lehtinen, K. E. J.; Carrier, M. J.; Zachariah, M. R. Structure and properties of silica nanoclusters at high temperatures. *Phys. Rev. B* **2002**, *65*, 235410.

(3) Applied Physics Letters. **1969**, *14*, 114.

(4) Nuclear Instruments and Methods. **1980**, *168*, 265–274.